

DOI: 10.11779/CJGE201404016

Physical model tests on expansive soil slopes

CHENG Zhan-lin¹, DING Jin-hua^{1,2}, RAO Xi-bao¹, CHENG Yong-hui¹, XU Han¹

(1. Yangtze River Scientific Research Institute, Key Laboratory of Geotechnical Mechanics and Engineering of the Ministry of Water

Resources, Wuhan 430010, China; 2. College of Civil Engineering and Architecture, Zhejiang University, Hangzhou 310027, China)

Abstract: A series of large-scale static model tests on a compacted expansive soil slope under artificial rainfall are conducted for real-time monitoring of water content and swelling deformation. The monitoring results show that the distribution of water content in the slope is nonuniform in space and time, which results in the nonuniform distribution of swelling deformation at the drying-wetting interface. According to the survey of failure surface by excavation after landslide, it is observed that local shear ruptures firstly take place at the drying-wetting interface within the shallow layer of slope, and then extend downwards gradually with water infiltration, and multiple shear sliding surfaces are produced at different depths and areas, which connect further with each other and finally lead to an overall landslide. The traditional limit equilibrium method can not correctly simulate the progressive landslide of expansive soil slopes. The finite element method with expansive model is adopted, and the safety factor of the model test slope is calculated to be 0.92 using the strength reduction technique. Both the physical model tests and the finite element analysis prove that the essential influence factor of expansive soil slope stability is the swelling deformation instead of the over-consolidation effect and fissure presence.

Key words: expansive soil; slope stability; physical model test; swelling deformation; unsaturation; FEM

CLC number: TU443

Document code: A

Article ID: 1000 - 4548(2014)04 - 0716 - 08

Biography: CHENG Zhan-lin (1963-), male, Professorate senior engineering. Major researches on geotechnical engineering and hydraulic engineering, especially on the engineering characteristics of the coarse-grained materials, computational soil mechanics and engineering treatment of expansive soils, etc. E-mail: chengzl@mail.crsri.cn.

膨胀土边坡物理模型试验研究

程展林¹, 丁金华^{1,2}, 饶锡保¹, 程永辉¹, 徐 晗¹

(1. 长江科学院水利部岩土力学与工程重点实验室, 湖北 武汉 430010; 2. 浙江大学建筑工程学院, 浙江 杭州 310027)

摘 要: 进行了一系列压实膨胀土的大型静力模型试验, 对边坡土体吸湿后的含水率、膨胀变形等进行了实时监测。试验成果显示, 膨胀土边坡浅层土体吸湿后其含水率场分布不均匀, 干湿分界面处土体易由于不均匀膨胀变形而导致局部剪切错动, 并随水分在坡体内的迁移, 局部滑动面逐渐向边坡纵深扩展, 在不同深度、不同部位形成多重剪切滑动面, 最终导致边坡整体塌滑。针对静力模型试验进行了考虑膨胀性的非线性有限元计算, 比较了边坡自重条件下和吸湿后应力场的变化, 可知吸湿引起顺坡向正应力在干湿分界面处变化剧烈, 剪应力明显增大, 强度折减法得到的模型试验边坡安全系数仅 0.92。研究成果表明: 影响膨胀土边坡浅层稳定性的最根本原因并非膨胀土的超固结性或裂隙性, 而是土的胀缩特性。

关键词: 膨胀土边坡; 模型试验; 膨胀变形; 渐进性破坏; 非饱和; 有限元分析

0 Introduction

The expansive soil (ES) is known as "trouble soil" or "expensive soil" because of the long-term potential instability, recurrent risk and high costs of maintenance. Geotechnical engineers summarized the special properties of ES, such as swelling-shrinkage behavior, fissure presence and over-consolidation effect, etc [1-3].

Lots of significant damages of geotechnical structures were induced worldwide by ES. China is one of the countries with a wide distribution of ES, and the ES

Foundation item: This research is financially supported by the National Key Technology R&D Program in the 11th Five-Year Plan of China (2006BAB04A10)

Received date: 2013 - 04 - 08

engineering problems are very serious^[4-6].

Slope failure, including landslide and collapse, can easily occur in expansive soil area. By means of investigation on large number of expansive soil slope (ESS) failure instances, the typical characteristics of landslide of ESS are summarized to be shallow layer (generally not more than 3 m), tractive sliding, gentle motion and seasonal occurrence, which are closely associated with swelling-shrinkage, crack and over-consolidation behavior of ES. Basma et al^[3] studied the swell-shrinkage behavior of expansive clays and considered that cyclic swelling process leads to a gradual destruction of the contacts in the clay structure. Zhan^[7-8] investigated the behavior of an unsaturated medium expansive clay and studied the failure mechanism of rain-induced landslips in the in-situ unsaturated expansive soil slope. There are some engineers who consider that failure of ESS is only caused by the strength reduction after several drying-wetting cycles, so the limit equilibrium method is still used to evaluate stability of ESS. But the safety factor which is calculated even using a smaller value than the residual strength of ES is still large, and disagrees with the fact that some filling expansive soil slopes slide after once rainfall^[9-11]. So, the strength reduction cannot fully explain the instability of ESS, and the soil strength is not the only key index in stability analysis.

During recent years, Yangtze River Scientific Research Institute (YRSRI) has been committed to the research on failure mechanism and treatment

technologies of ESS, which is closely related to South-to-North Water Transfer Project (SNWTP)^[12-15]. For this purpose, a series of laboratory experiments, large-scale static model tests, centrifugal model tests, numerical analyses and in-situ slope failure tests are performed. Some new viewpoints are formed concerning shallow progressive landslide and deep failure of ESS. This paper only focuses on the shallow landslide of compacted expansive soil slope which is irrespective of over-consolidation effect and swelling-shrinkage cracks, and mainly introduces the large-scale static model tests and the corresponding finite element analysis. From the test results and numerical analyses, the key effect of the swelling expansion on the shallow progressive failure process of ESS is revealed and analyzed.

1 Properties of compacted expansive soils

1.1 Basic physical properties

The expansive soils used in the static model tests are sampled from the channel of SNWTP in Handan, Hebei Province. Laboratory tests, complying with China's "Specification of Soil Test (SL237-1999)", are performed in order to evaluate physical properties of compacted expansive soils. Additionally, clay mineral composition is also assessed. From Table 1, it can be noted that the clay mineral is mostly montmorillonite with over 40 percent. The free-swelling index given by free swell tests is 124%, showing that the expansion degree of Handan expansive soils is high.

Table 1 Physical properties and mineral composition of expansive soils

Consistency limits		Grain size		Compaction	
Liquid limit/%	81.2	Silt (>0.005 mm)/%	52.2	Maximum dry unit weight, $\gamma_{dmax}/(kN \cdot m^{-3})$	16.8
Plastic limit /%	32.9	Fine silt (<0.005 mm)/%	47.8	Optimum water content, $w_{op}/\%$	19.9
Shrinkage limit/%	15.1	Clay (<0.002 mm)/%	30.8		
Plasticity index/%	48.3				
Natural field condition		Expansion		Percentage of total non-clay minerals	
Specific gravity, G_s	2.75	Free swelling index/%	124	Quartz/%	36
Water content, $w/\%$	33.0	Degree of expansion	High	Alkali feldspar/%	6
Dry unit weight, $\gamma_d/(kN \cdot m^{-3})$	13.9	Expansive force/kPa	64.6	Anorthose/%	11
Void ratio, e	0.998			Percentage of total clay minerals/%	
Saturation degree, $S_r/\%$	92.8			Montmorillonite/%	41
				Kaolinite/%	6
Soil classification:		CH			

1.2 Expansion

Huder-Amberg (1970) drew a conclusion that the relationship between expansion swelling and logarithm of expansion stress is linear through uniaxial expansion strain tests, and this linear law was proved by other scholars [16]. In this paper, for Handan ES, a series of triaxial swelling tests are conducted. The tests data show that the relationship between volume expansive ratio ε_v and mean principal stress σ_m can be generalized as:

$$\varepsilon_v = a + b \ln(1 + \sigma_m) \quad (1)$$

where, ε_v is the volume expansive ratio (%) caused by full moisture absorption of soil; σ_m is the mean principal stress (kPa); a , b are the coefficients related to initial moisture content. When the degree of compaction is 0.95 and the initial water content is 26% for Handan ES, $a=31.17$ and $b=-6.31$ (shown in Fig. 1).

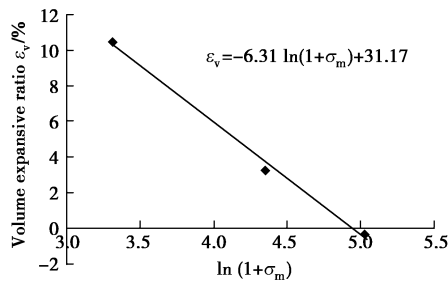


Fig. 1 Relationship between volume expansive ratio and stress by triaxial swelling test ($w_0 = 26\%$)

1.3 Mechanical properties

Fig. 2 shows the strength envelope of compacted expansive soils obtained from consolidated-drained triaxial tests. The strength parameters under high stress of 100~400 kPa are $c = 27.0$ kPa and $\varphi = 14.4^\circ$.

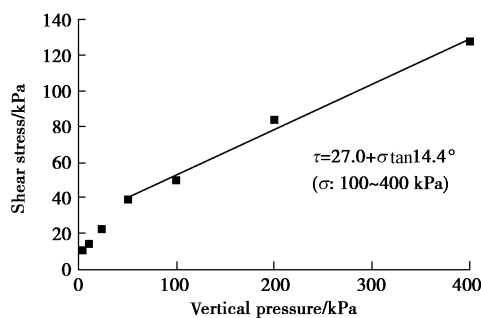


Fig. 2 Strength envelope of compacted expansive soils

2 Large-scale static model tests of expansive soil slopes

2.1 Overview of static model test system

The large-scale static model test system of YRSRI consists of a steel model box 6 m in length, 2 m in width

and 2.8 m in height, a loading system, an environmental simulation system and a measuring system. One lateral side of the model box is made of special glass so that slope failure process can be observed (see Fig. 3). The environmental simulation system includes a rainfall generator, an evaporation device and a set of water-supplying network. Artificial rainfall is generated by a group of spray nozzles which can control rainfall and rainfall pattern. Actual infiltration rate can be back-calculated by two flow meters installed at inlet pipe and outlet pipe with the diameter of 0.1 m. In addition, the measuring system can not only measure the real-time deformation, earth pressure, soil suction and water content, but also monitor water level, flow, temperature and slope runoff.

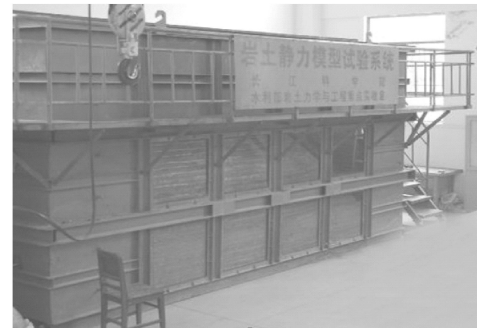


Fig. 3 Photo of large-scale static model test system of YRSRI

2.2 Test procedure and monitoring arrangement

Firstly, soil samples are prepared according to the initial moisture content of 20%, then compacted to the dry density of 1.60 g/cm^3 (degree of compaction is 0.95) using the layered roller compacted method. While dumping and compacting the soils, some necessary transducers are placed at the designated locations. After soil sample height reaches the specified value, test technicians shape it into a slope with a slope ratio of 1 : 1.5. Finally, displacement transducers and rainfall equipments are installed.

The test plans are listed in Table 2. The first test Q1-1 does not set the soil foundation and neglects the drainage of model box, and then the second test Q1-2 ameliorates the above two handicaps to study the effect of high rainfall on slope stability. The third test Q1-3 changes the rainfall ways and focuses on the slope stability under the condition of low-intensity continuing rainfall. In all the three model tests, landslides occur due to rainfall infiltration and the sliding processes are

Table 2 Static model test plans of compacted expansive soil slopes

No.	Soils	Slope sizes	Hydrologic conditions
Q1-1	Compacted	◆ without foundation	◆ without drainage in model box;
	high expansive soils	◆ slope ratio: 1: 1.5 ◆ height of slope: 2.5 m ◆ crest width: 2.5 m ◆ foundation thickness: 0.5 m	◆ high rainfall (the infiltration intensity of 1.7~8.1 mm/h) in range of slope surface
Q1-2	Compacted	◆ slope ratio: 1:1.5	◆ drainage in model box;
	high expansive soils	◆ height of slope: 2.0 m ◆ crest width: 1.75 m ◆ distance between the slope toe to box boundary: 0.85 m	◆ high rainfall (the infiltration intensity of 8.6~12.3 mm/h) in range of slope surface and the crest
Q1-3	Compacted high expansive soils	◆ the same as the test Q1-2	◆ drainage in model box; ◆ low-intensity continuing rainfall (average infiltration intensity of 0.53 mm/h)

similar. Therefore, in this paper, the test Q1-3 is mainly discussed and analyzed as a representative.

Fig. 4 shows a typical monitoring diagram for the test Q1-3. In test Q1-3, monitored variables mainly include moisture content and swelling deformation. The water content is obtained by two ways, one is to use the PR2 Profile Probe which can measure soil moisture over time at 4 depths down to 40 cm, and the other is by the drying method with drilled soil samples during the test process. In addition, the soil deformation is measured by some displacement transducers (LVDT) and inclinometer probes. All transducers are calibrated before tests. Moreover, some special landmarks are formed by filling black fine soils into drill holes at the cross-sectional profile after the slope model is shaped, that is to observe clearly the shear deformation status inside the slope. As the diameters of the drilling holes are very small and their depths are only 0.5 m, these landmarks in slope don't affect the slope integrity.

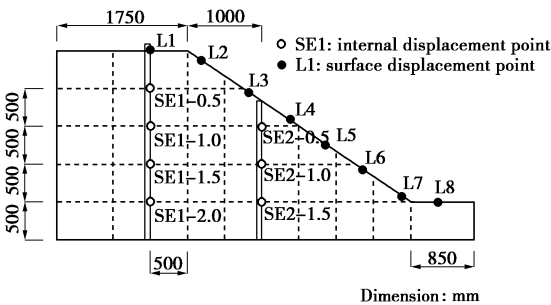


Fig. 4 Arrangement diagram of measuring instrument of static model test Q1-3.

2.3 Test results

2.3.1 Moisture content

The time step of rainfall distribution in test Q1-3 can be shown as follows:

0~12 h, 41~52 h, 108~153 h, 238~266 h, 338~341 h, and 360~363 h are the rainfall periods, and 12~41 h, 52~108 h, 153~238 h, 266~338 h, 341~360 h, and 363~385 h are the rainfall break periods.

The initial water contents at different depths of the compacted expansive soil slope are between 19.6% and 24.4%. The real-time water contents are obtained by drilling during tests. Fig. 5 shows the water content distribution with depth at different time.

The water content at shallow depth of 0.2 m increases rapidly to more than 30% in the first 100 h, and then keeps stable between 40% and 45%, which means that the soils are nearly saturated. With rainfall, water gradually infiltrates downwards. The water content at depth of 0.3~0.4 m at 238 h increases to more than 40%.

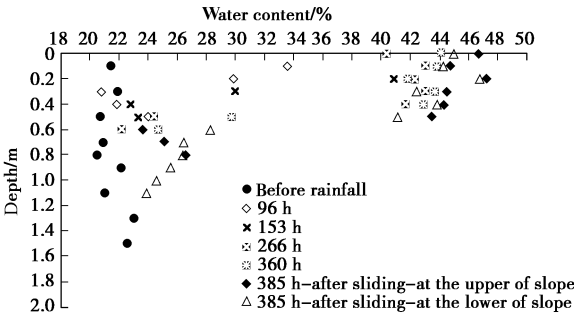


Fig. 5 Water content distribution of expansive soil slopes in test Q1-3

At the same time, many cracks are observed in the lower part of ESS through the glass side of the model box. Horizontal displacement of ESS is considerably

large and several tensile cracks also occur at the top of the slope. Further on, the water content at depth of 0.5 m changes significantly during 266 to 338 h. After occurrence of landslide at 385 h, the water content below depth of 0.6 m shows little change and almost maintains the initial value at the upside of landslide, but the infiltration depth is about 0.8 m at lower part of slope.

2.3.2 Swelling deformation

The displacement-time curves at some typical measuring points are shown in Fig. 6. The swelling deformation induced by rainfall infiltration shows the following characteristics:

(1) The continuous swelling deformation is in accordance with the variation process of soil water content. Moreover, the swelling deformation distributes nonuniformly in space and time. The deforming rate in the middle and lower parts of the slope is significantly larger than that in the other parts. The maximum swelling deformation at the measuring point L5 is about 82 mm.

(2) At the crest and shoulder of slope, expansive soil swells firstly with rainfall. But after a period of time, the soil water content at the shallow slope increases rapidly to near saturation and some tension cracks occur at the slope shoulder. Then the slope slides down, at this time, the soil displacement is shown as settlement.

(3) After landslide, the horizontal displacement in middle slope reaches about 20 cm, and about 10 cm at the top of slope.

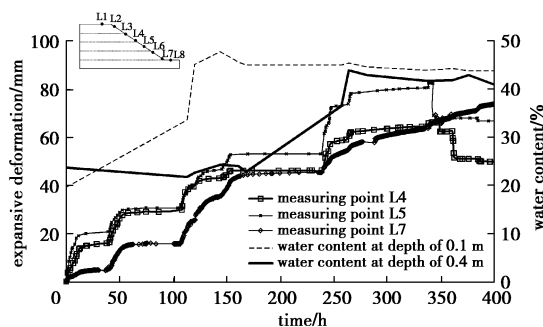


Fig. 6 Swelling deformation-time curves at typical measuring points of ESS

2.3.3 Slope failure

After rainfall for 27 h in test Q1-3, a crack is first formed in the lower part of the slope (about 0.5 m above the slope toe). Observed through the glass, with rainfall continuing, the crack develops further. At 257 h, many local tension cracks are clearly observed in the middle

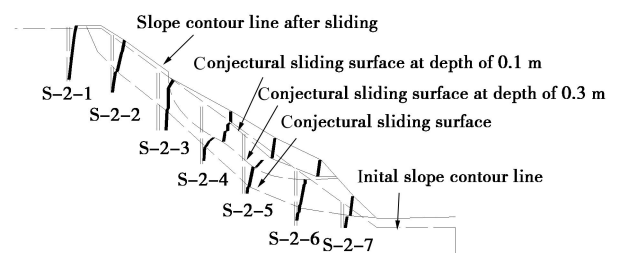
and lower parts of the slope. The horizontal displacement of the slope is visible and a penetrating crack at slope crest is formed. At 385 h, local collapse occurs in the lower slope where the first crack occurs. Afterwards, overall landslide is triggered and lasts for 2 min.

After sliding, the slope is excavated and some soil samples are taken near sliding surface for indoor tests. The test results show that the consolidated-drained shear strength of soil decreases to c_{CD} of 13.1 kPa and ϕ_{CD} of 6.2° .

In addition, by taking a picture and measuring the displacements of the special landmarks at the cross-sectional profile after excavation, the inner shear deformation of ESS can be shown in Fig. 7. It is clearly indicated that shear dislocations firstly occur in multiple shallow places of the slope, then develops further to connect with each other, and finally forms a large shear band.



(a) Photo of the axis profile



(b) Conjectural sliding surfaces

Fig. 7 Landslide of model test Q1-3

Sliding surfaces can be conjectured as shown in Fig.7(b). It is indicated that local sliding surface extends gradually from the shallow layer of the slope to a deep area, and finally forms a large-area collapse. Two obvious sliding surfaces are respectively at depths of 0.1 and 0.3 m. The maximum shearing displacement is up to about 20 cm at the depth of 0.3 m. Compared with those at the measuring point L5 and the landmark S-2-5(both positions are close), the swelling deformation and shear displacement are both larger.

2.3.4 Brief summary

The static model tests reflect visually some failure

characteristics of ESS, such as shallow sliding, progressive failure and tractive sliding behavior. For the layered roller compacted filling slope, there are no over-consolidation effect and swelling-shrinkage cracks induced by drying-wetting cycles. The nonuniform swelling deformation caused by water infiltration is thus the key reason for soil strength reduction and shallow sliding failure of ESS.

3 Finite element analysis with expansive model

At first, the safety factor of the slope of the static model test Q1-3 is calculated by the traditional limit equilibrium method. It is 5.2 under saturated shear strength of compacted ES (c_{CD} 27.0 kPa, φ_{CD} 14.4°), and even still 1.9 under shear strength after sliding (c_{CD} 13.1 kPa, φ_{CD} 6.2°). Both values of the safety factor do not agree with those under the sliding state of the model tests because the traditional limit equilibrium analysis model is based only on soil strength and the influence of the swelling deformation on slope stability can not be reflected. Therefore, the limit equilibrium method is unsuitable for analyzing shallow sliding failure of ESS.

In this paper, to further discuss the mechanism of the shallow landslide induced by swelling deformation, nonlinear finite element analysis for the static model test Q1-3 is carried out. The safety factor is calculated by using the strength reduction technique.

The ideal elastic-plastic model of ES and the Mohr-Coulomb failure criteria are used in ABAQUS finite element program. The soil strength parameters are shown in Table 3. The elastic modulus is defined by secant modulus corresponding to the peak strain because the failure of the expansive soil slope occurs at the shallow layer.

Table 3 Parameters of FEM analysis

Strength parameters		Wet density $\rho/(g \cdot cm^{-3})$	Elastic modulus /MPa	Poisson's ratio	Coefficient of expansive model	
c /kPa	$\varphi/(^{\circ})$				a	b
27.0	14.4	2.00	1.0	0.3	31.17	-6.31

To reflect correctly the expansion properties of ES in FEM, a hygroscopic area at shallow layer of ESS with depth of 0.5 m is simulated according to the static model tests. Then, the expansive model is adopted (see "expansion") to calculate the swelling deformation of ES induced by water content increasing from the initial

condition to the saturation. Afterwards, the swelling deformation is applied as the initial strain of each element in the designated area to iterate and get equivalent plastic strain distribution. According to the strength reduction technique, the safety factor of the slope is obtained when a yield surface forms, and for the model test Q1-3, it is 0.92. Fig. 8 shows stress contours and equivalent plastic strain distribution.

Comparing the difference of stress state between self-weight condition and moisture infiltration state, some knowledge can be acquired:

(1) By the expansive model adopted in this paper, it can be noted that changes of moisture content will clearly lead to stress field redistribution. Normal stress σ_x changes significantly at slope toe. Tangential stress σ_y increases in hygroscopic area and decreases in the lower part of the slope. Shear stress τ_{xy} is significantly larger at drying-wetting interface, and it changes obviously at the top and toe of the slope.

(2) The safety factor of model test slope is 0.92 calculated by FEM with expansive model and strength reduction method. It shows that FEM with expansive model can well agree with the model test results and is better than the traditional limit equilibrium method.

4 Shallow landslide mechanism of expansive soil slope caused by swelling deformation

By making static model tests and finite element analyses, the failure mechanism of shallow landslide of ESS can be discussed further.

Instability of ESS is closely related to change of hydraulic conditions. With rainfall infiltration, spatial and temporal distribution of water content of the slope is highly nonuniform. Soil water content at shallow layer of the slope increases quickly and forms a near saturation zone to prevent water from infiltrating to the deep area of the slope.

Due to the nonuniform spatial and temporal distribution of water content, the swelling deformation at different parts of slope doesn't synchronize even if expansive soils are homogeneously compacted and no cracks exist in the slope. At the drying-wetting interface, the swelling deformation is constrained, therefore large shear stress is produced and shear deformation becomes

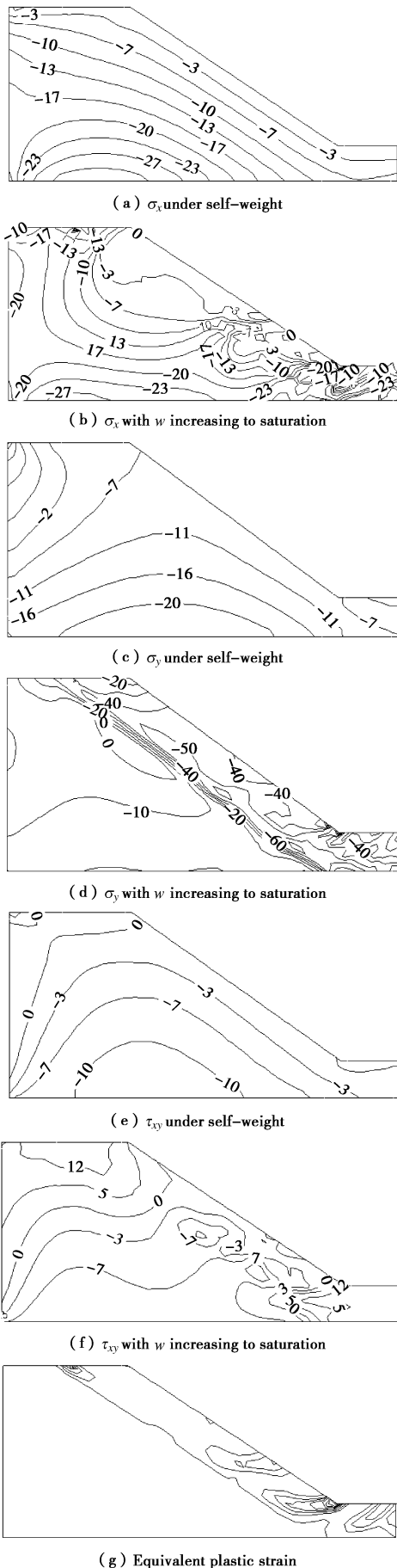


Fig. 8 Stress field and equivalent plastic strain of FEM of ESS

larger. When the local shear stress reaches the limit state, local failure will occur, as similar to the static model tests. Finally, multiple shear bands are connected with each other to trigger an overall landslide. Therefore, the characteristics of instability of shallow layer of ESS show obvious progressive tractive behavior.

5 Conclusions

Using a series of large-scale static model tests and nonlinear FEM with expansive model, the stability of shallow layer of expansive soil slopes is studied. A typical progressive sliding process is illustrated and analyzed properly. The main conclusions are drawn as follows:

(1) The failure mode of shallow sliding of expansive soil slopes can be named as the "shallow progressive landslide of ESS induced by swelling deformation". The key reason for the slope failure is nonuniform distribution of swelling deformation due to moisture infiltration, especially at the drying-wetting surface. It leads to slope stress field redistribution and strength reduction of expansive soils. Finally, local shear dislocation develops to form an overall landslide.

(2) For this type of shallow sliding of ESS induced by swelling deformation, the traditional limit equilibrium method is inapplicable. The finite element method with expansive model combined with the strength reduction technique can be more appropriate to properly evaluate the slope stability.

References:

- [1] SIVAPULLAIAH Puvvadi V, SITHARAM Thallak G, SUBBA RAO Kanakapura S. Modified free swell index for clays[J]. Geotechnical Testing Journal, 1987, **10**(2): 80 - 85.
- [2] GADRE A D, CHANDRASEKARAN V S. Swelling of black cotton soil using centrifuge modeling[J]. Journal of Geotechnical Engineering, 1994, **120**: 914 - 919.
- [3] BASMA Adnan A, AZM S A1-Homoud, Abdallah I Husein Malkawi, et al. Swelling-shrinkage behavior of natural expansive clays[J]. Applied Clay Science, 1996, **11**: 211 - 227.
- [4] LIAO Shi-wen. Expansive soil and railway engineering[M]. Beijing: China Railway Publishing Press, 1984.
- [5] LIU Te-hong. Expansive soil problems in engineering construction[M]. Beijing: China Architecture and Building

- Press, 1997.
- [6] SHI Bin, JIANG Hong-tao, LIU Zhi-bin, et al. Engineering geological characteristics of expansive soils in China[J]. Engineering Geology, 2002, **67**(1): 63 - 71.
- [7] ZHAN Liang-tong. Field and laboratory study of an unsaturated expansive soil associated with rain-induced slope instability[D]. Hong Kong: Hong Kong University of Science and Technology, 2003.
- [8] ZHAN Liang-tong, NG W.W Charles, BAO Cheng-gang, GONG Bi-wei. Artificial rainfall infiltration tests on a well Instrumented unsaturated expansive soil slope[J]. Rock and Soil Mechanics, 2003, **24**(4): 152 - 158.
- [9] YIN Hong-Lei, XU Qian-Jun, LI Zhong-Kui. Effect of swelling deformation on stability of expansive soil slope[J]. Rock and Soil Mechanics, 2009, **30**(8): 2506 - 2510.
- [10] YIN Zong-Ze, XU Bin. Slope stability of expansive soil under fissure influence[J]. Chinese Journal of Geotechnical Engineering, 2011, **33**(3): 454 - 459.
- [11] ZHOU Jian, XU Hong-zhong, HU Wen-jie. Impact of wetting-drying cycle effects on stability of expansive soil slopes[J]. Chinese Journal of Geotechnical Engineering, 2013, **35**(zk2): 152 - 156.
- [12] CHENG Zhan-lin, LI Qing-yun, GUO Xi-ling, et al. Study on the stability of expansive soil slope[J]. Journal of Yangtze River Scientific Research Institute, 2011, **28**(10): 3 - 111.
- [13] LI Qing-yun, CHENG Zhan-lin, GONG Bi-wei, et al. Failure mechanism and treatment technology of Expansive Soil Slope of Middle Route Project[J]. Journal of Yangtze River Scientific Research Institute, 2009, **26**(11): 1 - 9.
- [14] CHENG Yong-hui, LI Qing-yun, GONG Bi-wei, et al. Research of centrifuge modeling test on expansive clay slopes treatment effects[J]. Journal of Yangtze River Scientific Research Institute, 2009, **26**(11): 42-46, 51.
- [15] CHENG Yong-hui, CHENG Zhan-lin, ZHANG Yuan-bin. Centrifugal model tests on expansive soil slope under rainfall[J]. Chinese Journal of Geotechnical Engineering, 2011, **33**(S1): 409 - 414.
- [16] EINSTEIN H H. Suggested methods for laboratory testing of argillaceous swelling rocks[J]. Intl J of Rock Mech & Mining Sci & Geomechanic Abs, 1989, **26**(5): 415 - 426. (in Chinese)

首届全国文物建筑结构振动控制与保护学术会议 (1号通知 2014年10月 中国 西安)

我国是一个多地震国家,地震对现存文物建筑的结构安全构成了很大的威胁,尤其是2008年四川汶川大地震对文物建筑造成大面积的损坏后,地震和风振等对文物建筑的影响越来越受到社会各界的关注。随着我国经济的高速发展,工程建设与文物建筑的保护矛盾越来越突出,尤其是工业装备、铁路公路、城市轨道交通、工程施工等因素对文物建筑造成的振动影响越来越严重,对文物建筑的安全性将会带来很大的隐患。因此,评估地震、风振、工业振动、交通振动等对文物建筑的影响,采用经济合理适用的保护措施成为迫切需要解决的问题。

为交流总结近来我国在文物建筑振动控制的抗震方面的鉴定、评估、监测、修复、加固等方面取得的最新成果和经验,进一步推动其应用和学科发展,中国工程建设标准化协会建筑振动专业委员会文物建筑保护分会定于2014年10月在西安召开首届全国文物建筑结构振动控制与保护学术会议,同时召开分会成立大会。建筑振动专业委员会文物建筑保护分会及会议承办单位热忱期望全国相关专家、学者、工程技术人员和管理人员参加本次学术会议并发表学术论文,并欢迎有关企业在会议期间举办新技术、新产品展览。

主办单位: 中国工程建设标准化协会建筑振动专业委员会

文物建筑保护分会。

承办单位: 机械工业勘察设计研究院。

会议主题: 文物建筑的结构动力特性;文物建筑抗地震性能研究及工程实例;文物建筑抗风振性能研究及工程实例;文物建筑抗工业振动性能研究及工程实例;文物建筑抗交通振动性能研究及工程实例;文物建筑勘察技术;文物建筑监测技术;文物建筑评估与鉴定;文物建筑的隔振减振技术;文物建筑的修复加固技术。

论文征稿: 本次会议会前将正式出版论文集(或作为有关杂志增刊发表)作为会议资料,请拟提交论文的人员于2014年5月1日前提交论文题目和摘要,并在2014年7月1日前提交电子版论文全文。要求论文字数不超过6000字,文件格式为word文档。内容包括:论文题目、作者姓名、作者简介、作者单位(或联系方式)、论文摘要、关键词、正文、主要参考文献等。提交邮箱:wenwujianzhu@163.com。

会务组通讯地址: 西安市咸宁中路51号,机械工业勘察设计研究院;钱春宇:13572106623, 029-62658655;董霄:15191851914; E-mail: wenwujianzhu@163.com。

(大会组委会 供稿)